A Portable Sensing System for Impedance based Detection of Biotoxin Substances

V. I. Ogurtsov, K. Twomey and J. Pulka

Tyndall National Institute, Lee Maltings, University College Cork, Cork, Ireland

Abstract: The study describes the development of a portable autonomous biosensing platform for impedance based detection of biotoxin substances. The platform implements a label-free approach, which is based on detection of the biosensor interfacial changes due to a bio recognition reaction. The interfacial changes are sensed by means of Electrochemical Impedance Spectroscopy in a frequency range from 10 Hz to 100 kHz. The platform comprises of an electrochemical biosensor, portable low-noise mix signal hardware and associated software incorporating signal processing algorithms for extraction biotarget concentration from the biosensor response. The biosensor is realized as an on-chip package-free three electrode micro electrochemical cell consisted of a counter electrode (CE), a reference electrode (RE) and a working electrode (WE) patterned on a single silicon chip. WE represents an array of 40 um diameter gold disks with 400 μm center-to-center distance, which were undergone of corresponding surface modification for antibody immobilisation. The developed system was validated by an example of T-2 toxin detection. Performed calibration in the range of $0-250$ ppm of T2 toxin concentrations confirmed that the system can provide successful detection of the toxin at the levels below 25 ppm.

1 INTRODUCTION

Biosensing systems are increasingly used in a range of different applications including environmental, clinical, food, agriculture, and security (Bryan et al., 2013), (Zhang, Du, and Wang, 2015), (Wang, Lu, and Chen, 2014), (Yong et al., 2015). The conventional approaches are mainly lab-based and cannot be easily brought to the point-of-need. Modern microfabricated biosensors, on the other hand, offer the advantages of a cost-effective and rapid sample analysis, and specific and sensitive measurements over the more traditional methods, which tend to be multi-step (e.g. ELISA), or to involve sophisticated and expensive instruments (e.g. HPLC). The ability to apply semiconductor processing technologies, more commonly used in the IC industry, in the sensor chip fabrication (Herzog et al., 2013; Said et al., 2011) enables large batch production and subsequent availability of cheap and disposable devices. Typical microfabricated biosensors incorporate a gold electrode, or other e.g. platinum, Si_3N_4, active layer upon which different surface chemistries are applied to form a complete device that is specific and sensitive to a target of interest. There are different biosensor technologies Electrochemical, Optical, Thermal and Piezoelectric. Of these, the electrochemical biosensors accounted for the largest share of over 70% of the global biosensors market in 2013, which are expected to maintain their leading position during the forecast period from 2014 to 2020 (Transparency Market Research , 2014).

Within the branch of electrochemical sensors, there are amperometeric, potentiometric, impedimetric and field-effect transistor (FET) biosensors (Kafi et al., 2008), (Zhou et al., 2016), (Ogurtsov, Twomey, and Herzog, 2014). With the amperometric type biosensors, the changing current response is monitored with time; for the potentiometric the voltage is monitored. Both of these types offer a relatively straight forward measurement and a rapid analysis method. The impedimetric is more complex and more sensitive technique. Its classical implementation is based on the measurement of an AC current that forms in the response on the application to the sensor of a sinusoidal voltage over a set of frequencies.

There is a growing interest in label-free impedimetric biosensors due to such their advantages

as simplicity of sample preparation, high sensitivity and the ability to miniaturise the associated measurement instrumentation (Bryan et al., 2013), (Rushworth et al., 2014). A further advantage can be obtained by using of micro-sized electrodes, which improve the mass transport (and hence the sensor sensitivity) owing to the occurrence of radial diffusion over planar diffusion from macro-size electrodes resulting in an improvement in the signal-to-noise ratio and reduction in the iR drop (Arrigan, 2014).

The presented study describes the development of such portable immunosensing platform capable of biotoxin detection. The performance of the biosensing platform was validated by detection of T2-toxin. It is a trichothecene mycotoxin, which is toxic to humans and animals. It is naturally occurring mould byproduct of Fusarium spp. fungus that can be found in grains such as barley, wheat and oats.

2 EXPERIMENTAL

2.1 Description of the Bio Sensing System

The platform implements a label-free approach, which is based on detection of the biosensor interfacial changes due to a bio recognition reaction. The interfacial changes are sensed by Electrochemical Impedance Spectroscopy (EIS) technique (measurement of the biosensor complex impedance in a wide frequency range) (Lasia, 1999). The platform structure is shown in Figure 1.
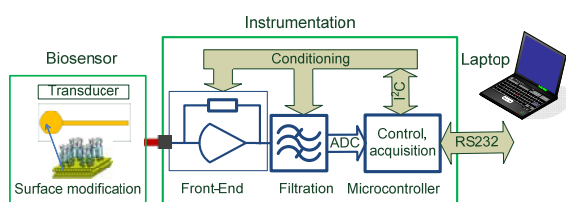

Figure 1: Structure of the biosensing platform.

It comprises of an electrochemical biosensor, low-noise mix signal portable instrumentation hardware and associated software incorporating signal processing algorithms for extraction biotarget concentration from the biosensor response.

2.1.1 Biosensor Chip

The biosensor is realized as an on-chip package-free three electrode micro electrochemical cell, which

includes a Pt counter electrode (CE), an Ag/AgCl reference electrode (RE) and an Au working electrode (WE) patterned on a single silicon chip as shown in Figure 2A, Figure 2B and Figure 2C. The WE represents an array (Figure 2B) consisted of 40 µm diameter recessed gold disks (Figure 2C) arranged in a hexagonal configuration with 400 µm center-to-center spacing, which were undergone of surface modification as will be described below. The WE was placed at the end of the chip to provide its separation from RE and CE. Such arrangement was implemented in order to facilitate the bio functionalization chemistry and prevent both RE and CE from interference with this process
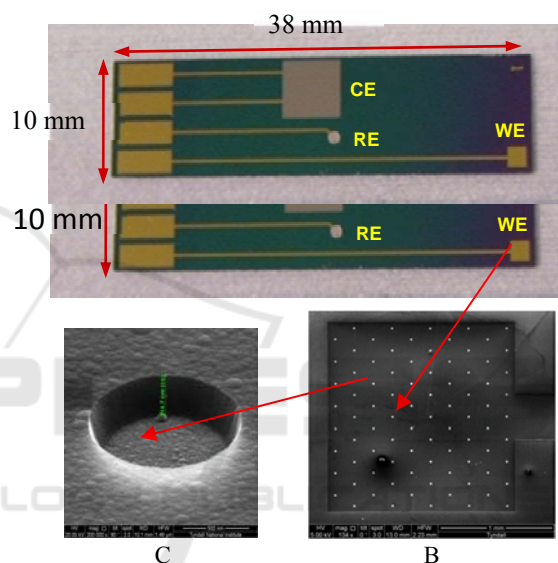

Figure 2: Photograph of an on-chip package-free three electrode micro electrochemical cell (A); SEM image of WE with 40 µm microdisk array (B) and SEM image of recessed gold disk produced by plasma etching of the silicon nitride isolation layer.

The on-chip micro electrochemical cell was fabricated at the Central Fabrication Facility at Tyndall National Institute. The electrodes on the on-chip microelectrochemical cell were patterned on a Si substrate of N-Type, <111>-orientation and fabricated by standard photolithography and lift-off techniques as described in (Said et al., 2011) and schematically shown in Figure 3. In brief, firstly, a silicon oxide layer of 1 µm thickness was thermally grown on the substrate and alignment marks were placed on the wafer. Then, the gold working electrodes, connecting tracks and pads of 150 nm thick, the platinum counter electrodes of 150 nm thick and silver reference electrodes of 250 nm thick were patterned on top of the silicon oxide layer by a

metal lift-off process. In this process 20 nm of Ti was used to promote the adhesion of the noble metals to the wafer that in case of Ag was supplemented by 20 nm of Ni. Then, 500 nm of silicon nitride was deposited on the whole wafer by plasma-enhanced chemical vapor deposition. The role of the silicon nitride is to insulate the connecting tracks from the solution. Openings for the electrodes and the connecting pads were obtained by plasma etching. Silver–silver chloride reference electrodes were prepared with help of chemical oxidation by immersion of the wafer in a 10 mM FeCl₃ solution for 50 s. The metal was then lifted and a resist layer was spin coated on top of the wafer to protect the electrodes during the dicing of the wafer into individual chips.
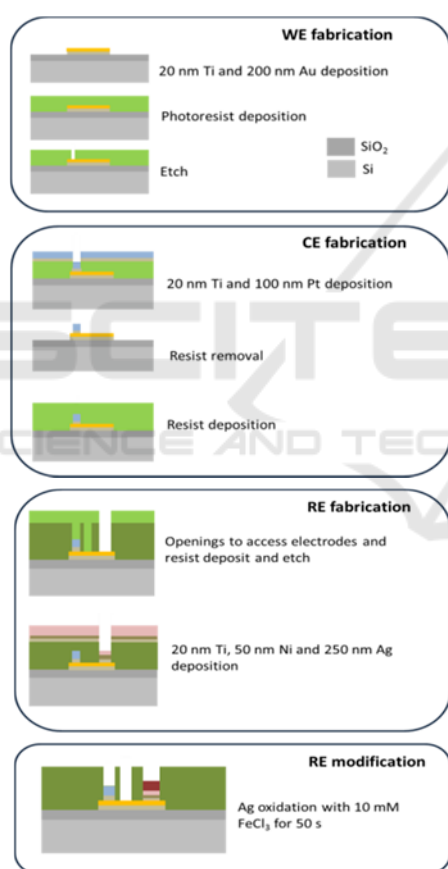

Figure 3: Fabrication process flow for the three electrode on-chip micro electrochemical cell.

2.1.2 Method and Chemicals

All electrochemical experiments were performed in a Faraday cage, and each measurement used for obtaining sensor calibration was carried out three times. EIS measurements were performed by the described system over a frequency range from 10 Hz to 100 kHz at an applied potential of DC bias of 0.2 V and an AC amplitude of 10 mV. The frequency range was defined by hardware specification and application objective to determine analyte concentration. The appropriate bias potential was determined from cyclic voltammetry over a range 0V to 0.6 V at a scan rate of 100 mV/s. All chemicals used in this work were purchased from Sigma Aldrich Ireland Ltd. and utilised as received.

2.1.3 Surface Modification Procedure

The working electrode of the microchemical cell was undergone of surface modification for attachment of antibodies capable of receipting the selected biotarget according to a scheme presented in Figure 4.
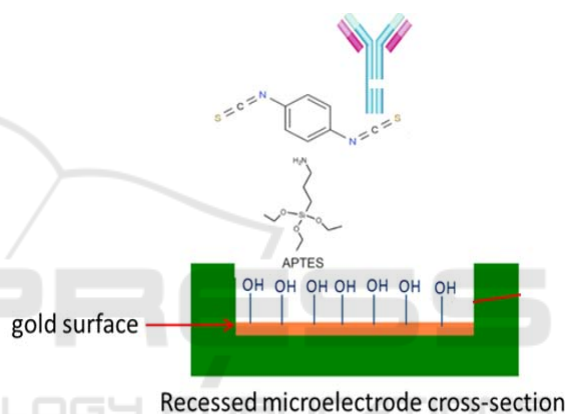

Figure 4: Surface modification scheme.

This procedure consisted of the following steps:

Electrode Surface Pretreatment. The fabricated chips were first plasma-cleaned for 10 minutes and then immersed in HCl:MeOH (1:1, v/v) solution for 15 minutes. They were then sonicated in acetone and isopropyl alcohol for 5 minutes each; rinsed with copious amounts of DI water and dry under a stream of nitrogen.

Silanisation of the WE surfaces was carried out in 3% APTES in MeOH:DI water (19:1) solution for 30 minutes at room temperature. The electrodes were then rinsed sequentially with MeOH and DI water before left cure in the oven (dust free) for 15 minutes at 120°C.

Surface Activation (Cross-Linker Attachment). Following the curing steps, the silanised electrodes were immediately immersed in 18 mL of DMF solution containing 2 mL of 10% pyridine and 0.098 g 1,4-phenylene diisothiocyanate (-PDITC) (produces 25mM PDITC) for 2 hours. The electrodes

56

were washed sequentially with DMF and DCE and dry under N_2.

Antibody Immobilisation. For this modification, anti-T2 toxin antibody was diluted in 0.1 M sodium borate pH 9.3. The working electrodes were immersed in 100 µL of diluted antibody solution for 2 hours at RT, wrapped in aluminium foil. Then the electrodes were removed, rinsed with DI water and dried with N_2.

2.1.4 Instrumentation

The instrumentation block diagram is shown in Figure 6. It represents a two channels EIS system where each channel contains a signal generator providing in-phase and quadrature AC signals, transimpedance amplifier and two (in-phase and quadrature) detection channels, each consisted of a mixer and a low-pass filter. These two paths are a sensor channel for the actual measurement and a reference channel to compensate for the background signal. The sensor connected to the reference channel should be not specific to the target analyte thereby capable of providing information on the sensor background signal resulting from varying parameters such as temperature, pH, nonspecific binding etc. If the background signal is of negligible value, the reference channel can be used as the second sensing channel for another bio target.

A known AC voltage that is generated by the signal generator is applied across the sensor and the sensor current is converted to a voltage by the corresponding transimpedance amplifier. The voltage is applied across the sensor and the sensor is amplified and demodulated in the I/Q demodulator yielding real and imaginary impedance components.

To increase the dynamic range of the module, 2-bit electronically controlled instrumentation amplifiers are included in the channel structure. To facilitate fine module adjustment and calibration, level shifters on the base of I^2C controlled DAC are introduced into the circuit.

The biosensing system hardware is realized consisted of two modules: Potentiostat and Front-End Amplifiers (PFEA) and Signal Processing and Microcontroller (SPM) units.

The PFEA (Figure 5) is designed as a separate small size unit in order to locate it close to a reservoir where the biosensor tests the sample solution.
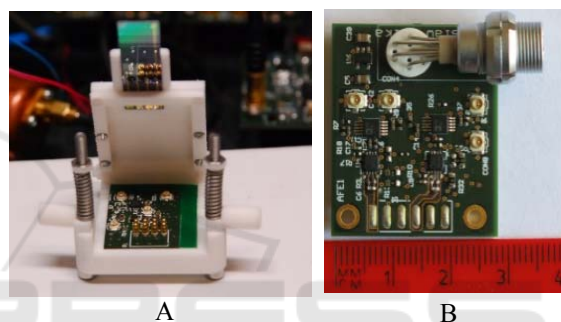

Figure 5: Potentiostat and Front-End Amplifiers module: photographs of the packaged unit with the sensor chip (A) and the unit PCB (B).
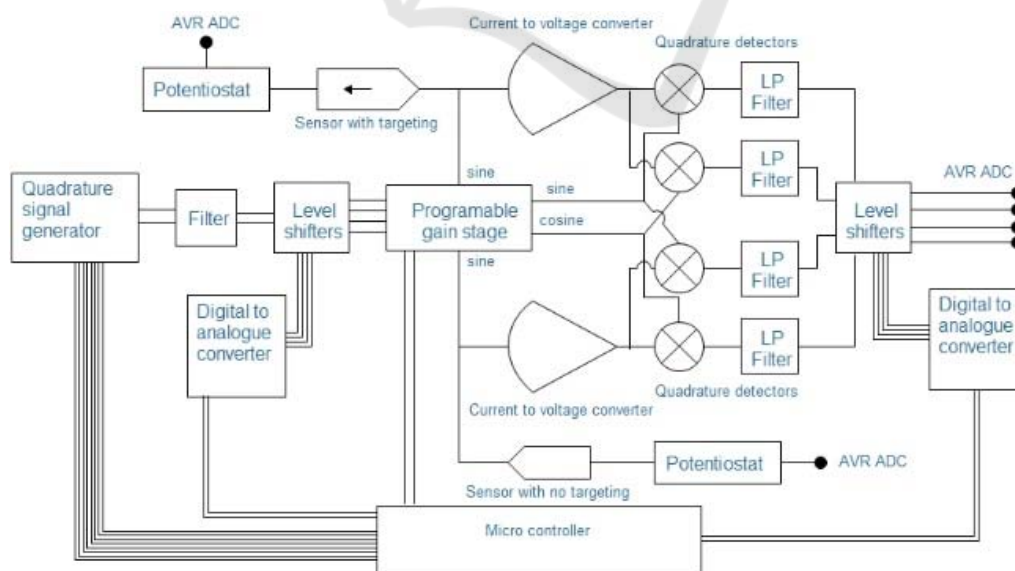

Figure 6: Instrumentation block diagram.

This shortens the length of the connection wires, which link the biosensor and front-end amplifier, therefore decreases the leakage current and attenuates the noise and electromagnetic interference. The PFEA unit consists of a potentiostat, a temperature sensor and two transimpedance amplifiers providing current to voltage transformation of the sensor and reference (calibration) signals. The potentiosat was realized on three operational amplifiers OPA2211. Two identical transimpedance amplifiers were assembled from OPAMP ADA4647 and instrumentation amplifier AD8253. The unit was implemented on a small four-layer PCB of 25 mm x 35 mm dimensions.

The Signal Processing and Microcontroller (SPM) unit (Figure 7) includes mixing and Analog Signal Processing (ASP), microcontroller and peripheral (µC) and Power Supply (PS) blocks.

Figure 7: Photograph of Signal Processing and Micro-controller unit.

The ASP block consists of Input, Switch, Level-Shifter and four identical Mixer/Low Pass Filter (LPF) lock-in circuits, which form two identical analog processing channels. Four-channel 16-bit digital to analog converters (DAC) incorporated into the SPM circuit is used to adjust DC levels in the SPM unit. The block was assembled from AD630 (Mixer), UAF42 (Low Pass Filter), ADG1419 (Switch), DAC8574 (DAC with buffered voltage output and I^2C compatible two wire serial interface), AD8253 (Instrumental amplifier with 2-bit electronically controlled gain) and LM4140 (1.024 V voltage reference).

The µC block is based on a high performance 8-bit ATxmega128A1U microcontroller. It realises functions of instrumentation control, data acquisition and communication. It also contains the signal generator and four 16-bit DACs. The signal generator is based on AD9854 chip, which is a DDS synthesizer

capable of parallel generation of precision sine and cosine signals.

The PS block supplies stabilised low noise voltages of +8V, -8V, +3.3V and -3.3V to power the signal generators, microcontroller, ASP and PFEA system units. The PS block can be powered from a voltage source in the range of +5V – +12V.

These three blocks formed the main body of the instrumentation were implemented in three separate 4 layer FR4 PCBs of 51 mm x 90 mm dimensions, which were integrated in a stack manner taking 55 mm of height as shown in Figure 7.

2.1.5 Signal Processing and Corresponding Software

The associated with instrumentation software consists of two highly interrelated parts written for a host computer and an ATxmega128A1U Atmel microcontroller. The software ensures communication between the instrumentation and the host computer, control of the instrumentation settings and its operation, implementation of the dedicated procedure of biosensor impedance spectra measurement and their signal processing. A smoothed differential impedance spectrum is used for extraction an analytical signal that is applied for biosensor calibration and quantification of the target analyte concentration. A developed automated procedure for analytical signal extraction includes the following steps: smoothing of the initial biosensor impedance spectrum by Kernel smoothing procedure; subtraction of a reference background spectrum from the measured spectra; and finally finding the maximum of the imaginary component of the differential impedance spectrum, which is taken as the analytical signal to be used for biosensor calibration and calculation of the target concentration (based on the biosensor calibration and extracted value of the analytical signal).

The PC software was implemented as user-friendly multi-tab GUI software where each tab is associated with the program window contained means for solutions of assigned tasks. There are three tabs/windows, namely 'Protocol', 'System configuration', and 'EIS'.

The tab/window 'Protocol' allowed for careful design of frequency sweep measurement protocol for each frequency point by applying values of frequency and measurement number with corresponding adjustment of all electronically controlled hardware parameters.
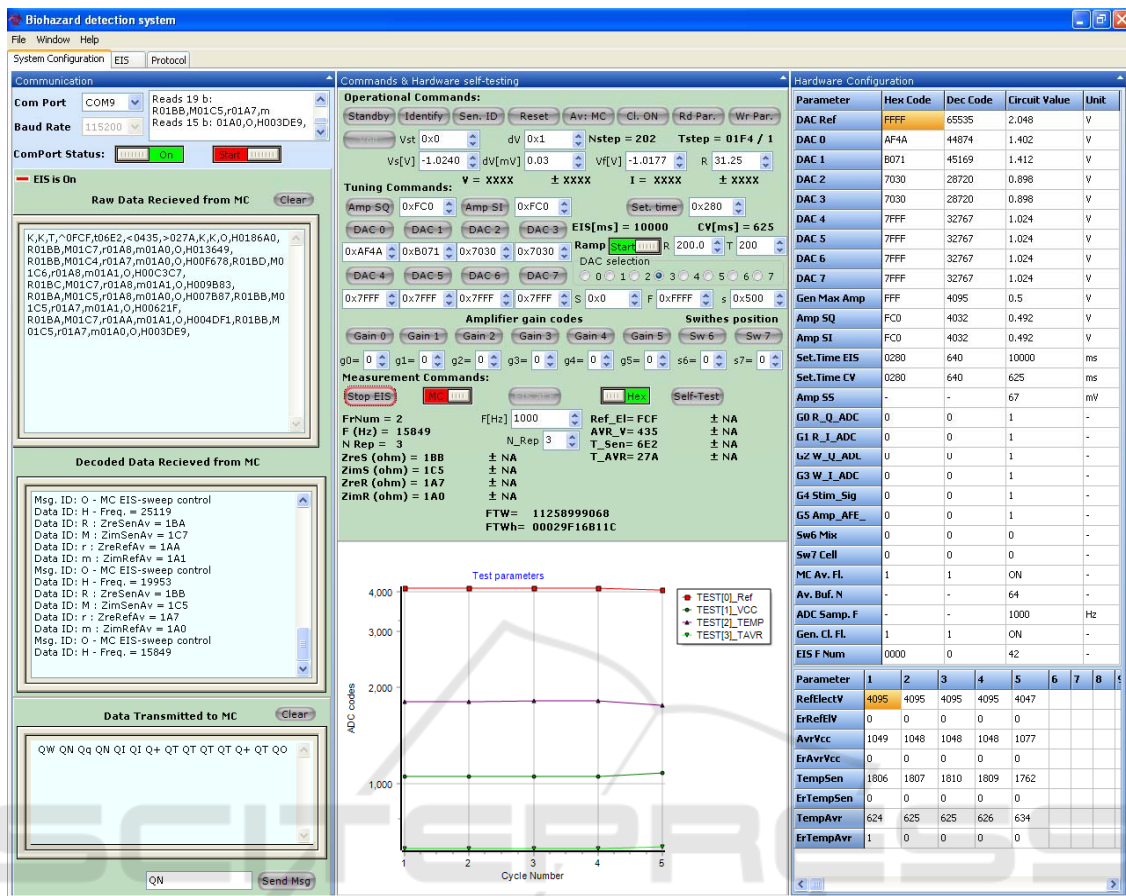
Figure 8: Screen short of System configuration PC software tab/window.

The tab/window 'System configuration' shown in Figure 8 provides communication control including received and transmitted data stream visualisation, detection and control of communication and stream errors, data extraction from communication stream, instrumentation and measurement setting control and configuration and system operability testing. Tools for system operability testing include Self-Test command, which starts Self-test measurement procedure followed by reporting about the measurement results in the 'Test parameters' plot and in the 'Test parameters' table in 'Hardware Configuration' panel. The program monitors these parameters before each impedance spectrum measurements that allows for easy identification of the hardware and the biosensor operability problem.

3 RESULTS AND DISCUSSION

The tab/window 'EIS' is the main instrumentation software part that is designed to provide all raw impedance measurements and signal processing results in different forms as shown in Figure 9. These include raw sensor impedance measurements presented by Nyquist (Imaginary impedance part vs. Real impedance part - 'Zim vs Zre') and Bode (Imaginary impedance part vs. Frequency - 'Zim vs F', Real impedance part vs. Frequency - 'Zre vs F' and Phase vs. Frequency - 'Phase vs F') plots as well as the processed Nyquist spectra obtained after Kernel smoothing and subtraction of the reference background spectrum from the measured spectra with analytical signal extraction (see the plot 'Zim vs Zre processed' where the analytical signals extracted are highlighted by red points on the corresponding processed impedance spectra) and calculated analyte concentration in respect to the biosensor calibration (plot 'Anal. Signal vs. Concentration') in both graphical and table forms.

The experimental results presented in Figure 9 were achieved with T-2 toxin biosensor described above, which was used for the developed system validation. Initial and differential raw and smoothed impedance spectra were obtained for five T2-toxin concentrations 0, 25, 50, 100 and 250 ppm. In order

Figure 9: Screen short of EIS PC software tab/window.

to provide better distinguishability of the spectra the measurements were made without repetitions thus zero measurement errors are shown in the corresponding table below the "Electrochemical measurement" panel. As one can see, the initial impedance spectra were subjected to noise and application of Kernel's smoothing allowed for effective noise suppression. Due to a relatively high low frequency boundary of the sweep range (10 Hz) the obtained impedance spectra accounted only for high and middle frequency parts of a depressed semicircle response of a microdisc electrode array associated with semi-infinite radial spherical diffusion. When toxin concentration increases, real and imaginary impedance parts both also increase that reflects a growth of a layer with targeted species captured by antibodies due the antibody-antigen binding reaction. If toxin concentration exceeds the certain level this impedance increase is saturated due to a depletion of the free antibodies capable of biorecognition reaction.

As follows from Bode plots the most difference between spectra corresponding to the different toxin concentrations is located in a low frequency range below 250 Hz. Here, the imaginary impedance values are about one order less than their real counterparts; they are also more sensitive to variation of T2 toxin concentration. If frequency increases, both impedance components decrease but the imaginary impedance stays relatively constant at the frequencies below 250 Hz where the influence of the toxin concentration on the biosensor impedance is the most noticeable. This frequency behaviour of the imaginary impedance of the biosensor leads to the fact that frequency dependence of the impedance phase represents unimodal smooth function with maximal values in the range of 56 – 62 degrees around the frequency of 1 kHz.

The dependence of imaginary impedance against toxin concentration becomes more apparent if to study the differential impedance spectra obtained by subtraction of the spectrum at zero concentration,

which is used as the reference background spectrum, from the impedance spectra corresponded to nonzero toxin concentrations. These smoothed differential impedance spectra are shown in the plot 'Zim vs Zre processed'. There are also highlighted by red points the maximum values of the imaginary impedances on the corresponding processed impedance spectra.

These values were used as the analytical signals related to calibration curve of the developed label-free impedance immunosensor. This curve is shown in the plot 'Anal. Signal vs. Concentration' together with the analytical signals automatically extracted from the smoothed differential impedance spectra presented by the red squares. The calibration curve represents a nonlinear function that reflects the competitive nature of the antibody-antigen binding reaction. Parameters of this calibration function defined by application of logarithmic regression analysis are given in Table 1.

Table 1: Calibration parameters of the biosensing system with T2 toxin biosensor.

Function	Slope	R^2	Error
$y = a \cdot \ln(x+b) + c$	$a = 2.412 \cdot 10^4$	0.977	$7.144 \cdot 10^3$

Based on these parameters and the extracted values of analytical signals corresponding T2 concentrations can be determined as presented in the right table in the Table panel in Figure 9. As follows from the calibration curve the developed biosensing portable system can successfully detect biotoxin at the levels below 25 ppm.

4 CONCLUSIONS

A portable biosensing platform for impedance based detection and quantification of biotoxin substances capable of operation in autonomous mode has been developed. The platform implements a label-free approach, which is based on detection of the biosensor interfacial changes due to a bio recognition reaction. The interfacial changes are sensed by means of Electrochemical Impedance Spectroscopy in a frequency range from 10 Hz to 100 kHz. The platform comprises of an electrochemical biosensor, portable low-noise mix signal hardware with embedded microcontroller and associated software incorporating hardware and measurement control together with signal processing algorithms for extraction biotarget concentration from the biosensor response. The biosensor is realized as an on-chip package-free three electrode micro electrochemical cell consisted of a Pt counter electrode, an Ag/AgCl reference electrode and an Au working electrode patterned on a single silicon chip. The WE represents an array of 40 μm diameter gold disks with 400 μm center-to-center distance, which were undergone of surface modification for antibody immobilisation. The surface modification was based on APTES – PDITC procedure. The instrumentation was realised as a two channel EIS system, which used in-phase and quadrature demodulation of AC signal for extraction of the real and imaginary impedance components. The biosensing system hardware consisted of two modules: Potentiostat and Front-End Amplifiers (PFEA) and Signal Processing and Microcontroller (SPM) units. The corresponding software capable of autonomous operation contains two interrelated parts written for the host computer and the embedded microcontroller. An automated procedure for analytical signal extraction consists of: smoothing of the initial biosensor impedance spectrum by Kernel smoothing procedure; subtraction of a reference background spectrum from the measured impedance spectrum; and extraction from differential impedance spectrum the maximum of the imaginary component, which is used as an analytical signal for biosensor calibration and calculation of the target analyte concentration. The PC software was implemented as user-friendly multi-tab GUI software where each tab is associated with the program window. These are 'System configuration', 'Protocol' and 'EIS' tabs/windows. They provide communication, instrumentation and measurement setting control, and system operability testing; allow for design of impedance measurement protocol for each frequency sweep point; and present results of EIS and analyte concentration quantification in graphical and table forms. The developed biosensing system was validated with the developed on-chip T2 toxin biosensor. Calibration of the system was obtained for five toxin concentrations from 0 ppm to 250 ppm. It showed that the developed portable biosensing system can provide successful detection of the biotoxin at the levels below 25 ppm.

ACKNOWLEDGEMENTS

REFERENCES

Bryan, T., Luo, X., Bueno, P.R. and Davis, J.J. (2013) 'An optimised electrochemical biosensor for the label-free detection of C-reactive protein in blood', *Biosensors and Bioelectronics*, 39(1), pp. 94–98.

Zhang, W., Du, Y. and Wang, M.L. (2015) 'Noninvasive glucose monitoring using saliva nano-biosensor', *Sensing and Bio-Sensing Research*, 4, pp. 23–29.

Wang, X., Lu, X. and Chen, J. (2014) 'Development of biosensor technologies for analysis of environmental contaminants', *Trends in Environmental Analytical Chemistry*, 2, pp. 25–32.

Yong, D., Liu, C., Zhu, C., Yu, D., Liu, L., Zhai, J. and Dong, S. (2015) 'Detecting total toxicity in water using a mediated biosensor system with flow injection', *Chemosphere*, 139, pp. 109–116.

Herzog, G., Moujahid, W., Twomey, K., Lyons, C. and Ogurtsov, V.I. (2013) 'On-chip electrochemical microsystems for measurements of copper and conductivity in artificial seawater', *Talanta*, 116, pp. 26–32.

Said, N.A.M., Twomey, K., Ogurtsov, V.I., Arrigan, D.W.M. and Herzog, G. (2011) 'Fabrication and Electrochemical characterization of micro- and Nanoelectrode arrays for sensor applications', *Journal of Physics: Conference Series*, 307, p. 012052.

Transparency Market Research (2014) '*Global Biosensors market - industry analysis, size, share, growth, trends and forecast 2014-2020*', Available at: http://www.transparencymarketresearch.com/biosensors-market.html (Accessed: 15 December 2016).

Kafi, A.K.M., Lee, D.-Y., Park, S.-H. and Kwon, Y.-S. (2008) 'Potential application of hemoglobin as an alternative to peroxidase in a phenol biosensor', *Thin Solid Films*, 516(9), pp. 2816–2821.

Cheng, S., Hideshima, S., Kuroiwa, S., Nakanishi, T. and Osaka, T. (2015) 'Label-free detection of tumor markers using field effect transistor (FET)-based biosensors for lung cancer diagnosis', *Sensors and Actuators B: Chemical*, 212, pp. 329–334.

Ramesh, R., Puhazhendi, P., Kumar, J., Gowthaman, M.K., D'Souza, S.F. and Kamini, N.R. (2015) 'Potentiometric biosensor for determination of urea in milk using immobilized Arthrobacter creatinolyticus urease', *Materials Science and Engineering: C*, 49, pp. 786–792.

Zhou, Y., Tang, L., Zeng, G., Zhang, C., Xie, X., Liu, Y., Wang, J., Tang, J., Zhang, Y. and Deng, Y. (2016) 'Label free detection of lead using impedimetric sensor based on ordered mesoporous carbon–gold nanoparticles and DNAzyme catalytic beacons', *Talanta*, 146, pp. 641–647.

Ogurtsov, V.I., Twomey, K. and Herzog, G. (2014) 'Development of an Electrochemical Sensing System for Environmental Monitoring of Port Water Quality to Integrate On-board an Autonomous Robotic Fish.', in Hashmi, S. (ed.) *Comprehensive materials processing. Volume 13: Sensor Materials, Technologies and Applications*. Oxford, United Kingdom: Elsevier Science, pp. 317–351.

Bryan, T., Luo, X., Bueno, P.R. and Davis, J.J. (2013) 'An optimised electrochemical biosensor for the label-free detection of C-reactive protein in blood', *Biosensors and Bioelectronics*, 39(1), pp. 94–98.

Rushworth, J.V., Ahmed, A., Griffiths, H.H., Pollock, N.M., Hooper, N.M. and Millner, P.A. (2014) 'A label-free electrical impedimetric biosensor for the specific detection of Alzheimer's amyloid-beta oligomers', *Biosensors and Bioelectronics*, 56, pp. 83–90.

Arrigan, D.W.M. (2004) 'Nanoelectrodes, nanoelectrode arrays and their applications', *The Analyst*, 129(12), pp. 1157-1165.

Lasia, A. (1999) 'Electrochemical Impedance Spectroscopy and Its Applications', in Conway, B.E., Bockris, J., and White, R.E. (eds.) *Modern Aspects of Electrochemistry, Volume 32*. New York: Kluwer Academic/Plenum Publishers, pp. 143–248.